



Pure water production from aqueous solution containing low concentration hardness ions by electrodeionization

Yulong Su, Jianyou Wang*, Lin Fu

College of Environmental Science and Engineering, Nankai University, Tianjin 300071, China
Tel. +86 22 66229536; Fax: +86 22 66229563; email: wangjy72@nankai.edu.cn

Received 29 July 2009; Accepted 19 April 2010

ABSTRACT

The integrated membrane process of “reverse osmosis-electrodeionization (RO/EDI)” has been widely used for pure water production in recent years. However, in most cases, a single pass RO system still can not meet the feed standards of EDI, therefore the “RO/RO” system should be applied for scale averting. In this paper, a specially designed EDI process was developed with improvements on resins packing and inner configuration, and performances of six EDI stacks with different inner configurations were investigated and compared with each other. When with feed hardness of $11.7 \text{ mg} \cdot \text{L}^{-1}$ (as CaCO_3), the improved EDI process could give a hardness rejection of 99.8% while the energy consumption was as low as $0.26 \text{ KW} \cdot \text{h} \cdot \text{m}^{-3}$, and the steady product resistivity that could be achieved was $14.6 \text{ M}\Omega \cdot \text{cm}$. In durative experiment of 130 hours, the EDI had been operated with good stability and without precipitation.

Keywords: Electrodeionization; Hardness ions; Resins; Water dissociation

1. Introduction

Electrodeionization (EDI), which combines electrodialysis and ion exchange resins, is a hybrid deep desalting technology for pure water production. Owing to advantages such as continuous operation, high efficiency and no chemical regeneration, EDI has found its wide application in power, microelectronics, pharmaceutical and many other industries.

However, there are still some limitations of the current technology, the most important issue of which focuses on the feed quality. For high-purity water production, the method of polarity reversal, which is frequently used in conventional electrodialysis (ED), is not suitable for EDI process [1,2]. To avoid the precipitation problem, the feed quality and operation parameters

must be strictly restricted. As to the hardness, the value must be lower than $1.0 \text{ mg} \cdot \text{L}^{-1}$ (as CaCO_3). In practice, dual pass reverse osmosis (RO/RO) should be applied as pretreatment for EDI to constitute “RO/RO/EDI” integrated membrane processes, therefore the complexity and investment of the system will be both increased.

There have been some work reported by Tessier (2000) and Park (2007) of relaxing the feed limitations of the EDI [3,4]. We [5] have also reported that out dilute resistivity of $3.45 \text{ MW} \cdot \text{cm}$ was obtained with feed Ca^{2+} concentration of $5.0 \text{ mg} \cdot \text{L}^{-1}$. In this study, our purpose focuses on some new improvements for precipitation averting with feed hardness of up to $10 \text{ mg} \cdot \text{L}^{-1}$ (as CaCO_3). First, mixed-bed ion exchange resins, in which the volumetric proportion of cation resin was higher than 50%, were packed in concentrating compartments instead of layered polypropylene meshes; second, a specific inner flow circuit could be

*Corresponding author.

adopted, according to which the dilute stream had two passages while the concentrate stream just had one passage. For the dilute stream, the detention time was long enough to ensure electrolyte rejection; while as to concentrate stream, it could be effused out of the stack quickly. Series of experiments should be performed on different EDI stacks with different inner configurations to affirm the validity of the improvements.

2. Experimental

2.1. Materials

The cation and anion exchange membranes used, provided by Zhejiang Qianqiu environmental water treatment Co. Ltd., China, were both of heterogeneous type and with functionality of sulfonic acid and quaternary ammonium, respectively. The gel-type strong acid cation exchange resins of sodium form, named "001 × 7", and gel-type strong alkali anion exchange resins of chloride form, named "201 × 7", obtained from the chemical plant of Nankai University, Tianjin, China, were used for packing in the compartments. Prior to each experiment, the

resins were immersed in alcohol solutions for at least 24 h to remove potential impurities, and then washed with pure water till no alcohol remained.

2.2. Configurations of membrane stacks

Six laboratory EDI stacks with four different inner configurations were developed to evaluate the performances of deionization and precipitation averting. Each stack has four dilute compartments and five concentrate compartments in all, mixed-bed resins with volumetric ratio of 6:4 (anion to cation) were packed in dilute compartments. The inner configurations of these stacks are shown in Fig. 1.

Both the dilute and concentrate streams in configuration A have two flow passages, and the two flow directions were parallel each other. All the dilute, concentrate and electrode streams were flown from the anode side to the cathode side, and no resins but two-layered polypropylene screens were packed in concentrate compartments. As to other four configurations, the concentrate compartments were also packed with mixed-bed resins, while the volumetric ratio (anion to cation) of configuration B was 6:4, and that of configuration C, D and E were 1:3.

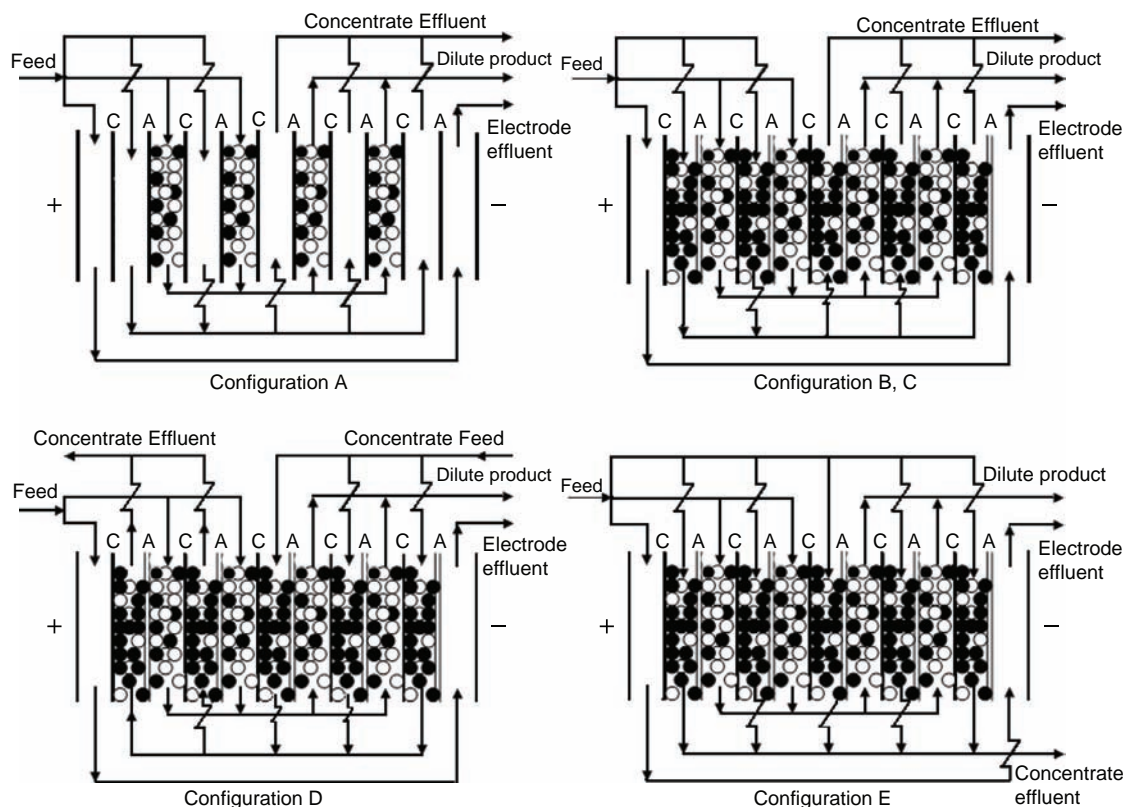


Fig. 1. Inner configurations of the EDI stacks. A: anion exchange membrane; C: cation exchange membrane.

Compared with configuration C, the flow directions of dilute and concentrate streams of configuration D were opposite to each other in each passage. The concentrate stream was flown from the cathode side to the anode side.

In configuration E, there were two flow passages for the dilute stream but only one for the concentrate stream. Directions of the two streams were parallel with each other in the first passage near dilute inlet but opposite in the second passage near dilute outlet.

Each chamber of the EDI units was 30.0 cm in length and 10.0 cm in width. Thickness of dilute and concentrate chambers filled with resins were both 3.0 mm, but that of concentrate chambers in the stack with configuration A was only 0.9 mm. Effective area of each membrane was 158.4 cm² (7.2 cm × 22 cm). The anode and cathode plates were made of ruthenium-coated titanium and stainless steel, respectively.

2.3. Experimental system

The flow diagram of the EDI system is illustrated in Fig. 2.

Feed water was first pressurized by the lift pump, and then divided into three currents as feed of dilute, concentrate and electrode streams. All three streams were flown directly through the stack without circulation. The out dilute stream was then collected as purified product while the concentrate and electrode effluents were discharged. Parameters such as pressure, pH, conductivity and resistivity of dilute and concentrate streams entered or exited the stack, were monitored by on-line monitors.

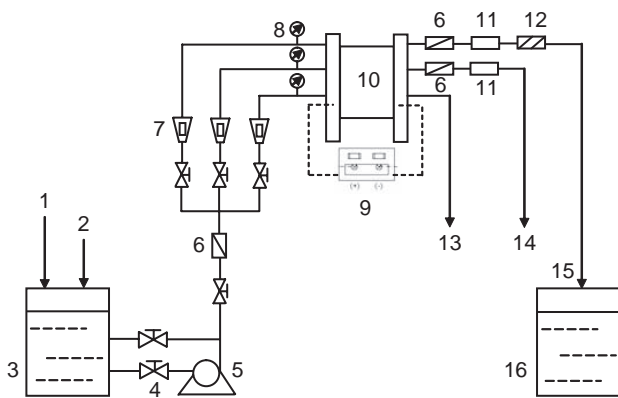


Fig. 2. Flow diagram of the EDI system. 1. RO permeate; 2. Hardness accession; 3. Feed tank; 4. Regulating valve; 5. Lift pump; 6. On-line Conductivity monitor; 7. Flow meter; 8. Pressure gauge; 9. DC Power supply; 10. EDI stack; 11. On-line pH monitor; 12. On-line Resistivity monitor; 13. Electrode effluent; 14. Concentrate effluent; 15. Dilute product; 16. Pure water tank.

2.4. Operation conditions

In all experiments, the feed water was prepared with previous RO product water by dosing CaCl₂ and MgCl₂. The concentration of Ca²⁺ and Mg²⁺ ions in feed were 3.0 mg·l⁻¹ and 1.0 mg·l⁻¹, respectively, thus the feed water had the conductivity of 32–33 μS·cm⁻¹ and hardness of 11.7 mg·l⁻¹ (as CaCO₃), which was similar with that in our previous work [5].

All experiments except the I-V curve investigation, were performed in potentiostatic model of 30 volts. The flow rate of dilute, concentrate and electrode stream were 30 l·h⁻¹, 6.0 l·h⁻¹ and 2.0 l·h⁻¹, respectively. Concentration of hardness ions (Ca²⁺ and Mg²⁺) were analyzed by ion chromatography (DX 120, Dionex Corp., US) equipped with an IonPac CG12, a CS12 analytical column, and a cation self-regeneration suppressor. Methanesulfonic acid, with concentration of 20 mmol·dm⁻³ and flow rate of 1.0 ml·min⁻¹, was applied as the eluate.

3. Results and discussion

3.1. Principle of precipitation averting

Compounds that contributed to precipitation in EDI process are mostly inorganics containing hardness ions such as CaCO₃, Mg(OH)₂, Ca(OH)₂ and MgCO₃. In general, it initially formed in concentrate compartments, especially on the surface of anion exchange membranes near the outlet, which is shown in Fig. 3.

The Ca²⁺ and Mg²⁺ ions in concentrate compartments come from the concentrate feed and the dilute compartments. It is obvious, if dilute and concentrate streams are in the same flow directions, then hardness concentration in concentrate compartments will continuously accumulate along with the stream. Since severe water decomposition, which would consequentially result in high OH⁻ concentration at local region in concentrate compartments, would take place especially downstream in dilute compartments,

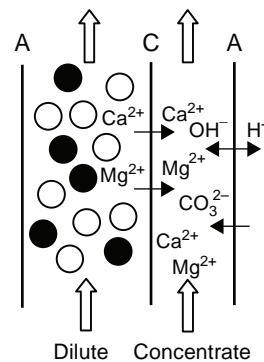


Fig. 3. Scaling formation in concentrate compartment.

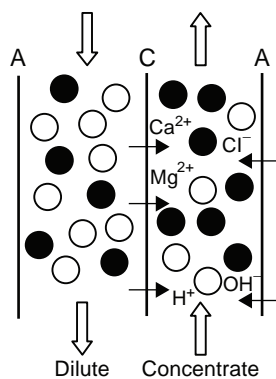


Fig. 4. Principle of precipitation averting.

therefore both high concentration of OH^- and hardness ions would further cause the scaling problem.

In our opinion, the countercurrent of streams and packing resins in concentrate compartments could be helpful to avert precipitation (Fig. 4).

First, after migration into concentrate compartments, hardness ions could be effused out of the stack via concentrate stream quickly. Second, since mixed-bed resins are filled in concentrate compartments, the cation exchange resins would restrain the OH^- ion from approaching the cation exchange membranes, while the Ca^{2+} and Mg^{2+} ions would also be baffled by the anion exchange resins. Besides, compared with filling layered screens, the distance between the membranes was evidently widened since mixed-bed resins were packed, therefore more detention time should be required for combination of OH^- and hardness ions, thus the precipitation was more difficult to take place in the concentrate compartments.

In all stacks described in section 2.2, there were two flow passages for the dilute stream to ensure enough hydraulic retention time for electrolyte rejection. Since water splitting takes place severely downstream, the second passage of dilute stream is then selected for the countercurrent arrangement.

Based on the above analysis, the stack with configuration E is considered to have the best capabilities of separation, which has been verified by the following experiments.

3.2. *I-V* curve investigation

To investigate the essential characteristics and performances of the improved EDI process, the *I-V* and *R-V* curves were explored via a new assembled stack with inner configuration of type E, which were demonstrated in Fig. 5.

It can be seen that there are three turning points both on the *I-V* and *R-V* curves, the corresponding voltage of

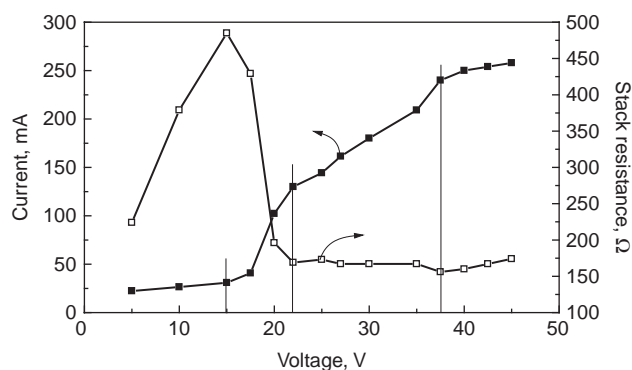


Fig. 5. *I-V* and *R-V* characteristics of the improved EDI process.

which are 15.0 V, 22.0 V and 37.5 V, respectively. With an increased applied voltage from 5.0 V to 15.0 V, the stack resistance climbed rapidly from 224 Ω to 485 Ω . In this region, the stack current increased very slightly along with the voltage, which was similar with that in a conventional ED process. The reason is that the resistance at the membrane-solution interface in dilute compartments increased significantly due to concentration polarization. In range of 15.0–22.0 V, the trend was reversed, the current increased remarkably while the resistance fell down to 169 Ω rapidly, which indicated significant water splitting reaction in dilute compartments.

When applied voltage was between 22.0–35.0 V, the current increased linearly along with the voltage, and the stack resistance kept stable at 167–173 Ω , which was nearly the lowest value on the *R-V* curve. In this region, as applied voltage increased, resistance of dilute compartments increased accordingly nevertheless that of concentrate compartments decreased, which further indicated increasing migration of salt ions into concentrate streams. The H^+ and OH^- ions produced by water dissociation were both available for resins regeneration and electrical current transport, thus the stack conductivity was enhanced.

When under applied voltage higher than 37.5 V, the stack resistance gradually increased again. The reason was that the increase amplitude of resistance of dilute compartments was greater than the decrease amplitude of concentrate compartments, most of the energy was consumed on water decomposition instead of salt ions migration.

According to Fig. 5, the applied voltage of 30.0–35.0 V was considered to be ideal for the operation. Since the potential hazard of precipitation would be more serious when under higher voltage, the voltage of 30.0 V was then selected for the applied voltage of continuous operation.

What should be noted is that the *I-V* curve investigation was carried out on a new assembled stack, and the virtual stable status had not been achieved yet till

termination of the experiment. If that operation continued under a certain voltage, the current would increase gradually, yet the I - V and R - V relationship should be also similar with that in Fig. 5.

3.3. Influences of stack configuration

3.3.1. Effects of resins packing in concentrate compartments

Three experiments were performed to evaluate the influences on separation of resins packing in concentrate compartments via three EDI stacks with configurations A, B, and C, the corresponding serial number of which were A1, A2, and A3, respectively. The pH of out dilute and concentrate streams, stack currents, and product resistivities of these experiments are shown in Figs. 6, 7 and 8.

It can be seen that, during 65 h operation after start-up, the variation of dilute pH of all experiments are similar with each other. The values kept stable around 8.0–8.5. However, dilute pH of experiment A1 dropped

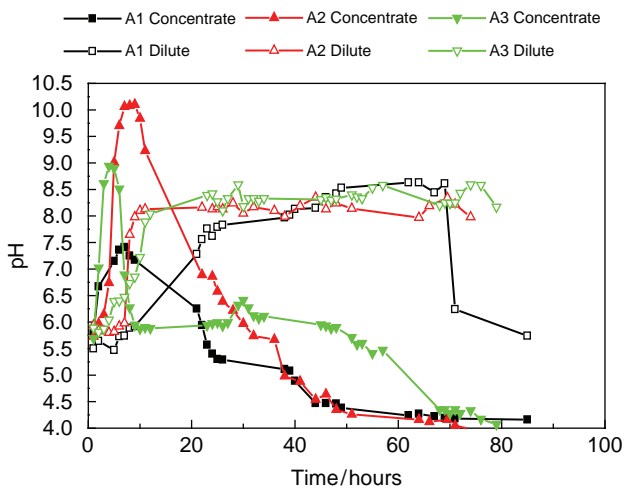


Fig. 6. pH of dilute and concentrate streams versus operation time.

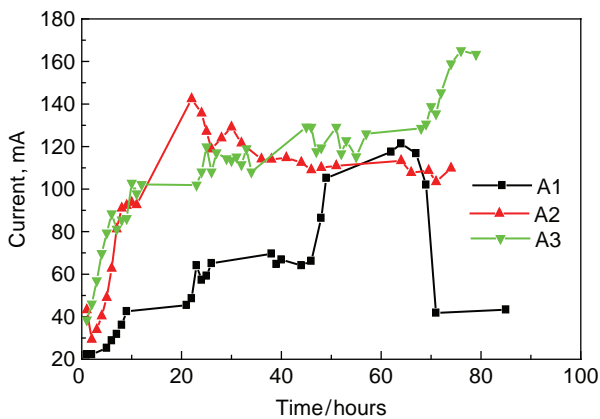


Fig. 7. Variation of stack currents versus operation time of different stacks.

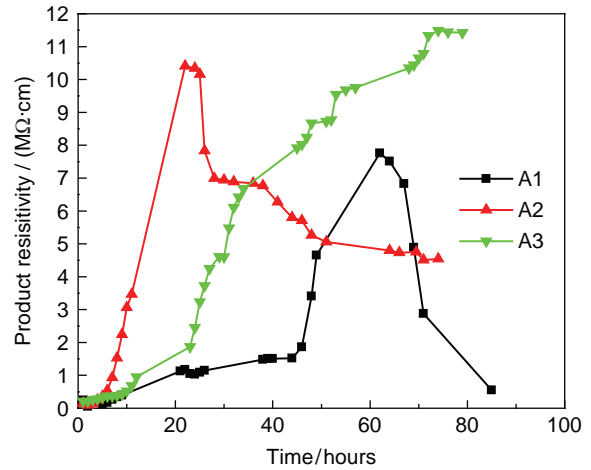
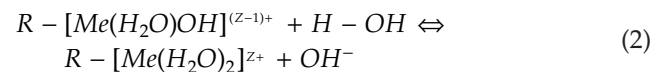
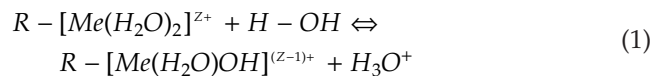


Fig. 8. Variation of product resistivity versus operation time of different stacks.

rapidly in the last 20 hours, which indicated that water decomposition took place acutely at the “anion exchange membrane-solution” interface in dilute compartments. Besides, from Figs. 7 and 8 it is also obvious, that the corresponding stack current of experiment A1 decreased notably after 62 h operation, and the dilute resistivity continuously fell down from 7.76 to 0.55 $M\Omega \cdot cm$, which both indicated serious precipitation had brought forth in the stack.

After 70 h operation, the concentrate pH of experiment A1 still kept at low level of 4.16–4.24 instead of evident increase. The reason is that there was a hysteresis for pH variation, and much of the OH^- ion migrated from dilute compartments had combined with hardness ions to form precipitation.

From Fig. 6 we could also come to some verdicts on mechanism of water decomposition. In each experiment, water splitting reaction occurred first on the surface of anion exchange membranes, which resulted in a transitory pH increase of concentrate stream in several hours after start-up. After the first period, the concentrate pH decreased rapidly since severe water splitting reaction also subsequently took place on the surface of cation exchange membranes, especially at the presence of hardness ions which could accelerate the split reaction greatly [6–8]. It has been reported that many metal ions, including Ca^{2+} and Mg^{2+} , could act as catalyst in the water splitting reaction according to the following mechanism [9,10]:



where R is the fixed functional group of the membrane and Me^{z+} is multivalent metal ion.

In EDI process, hardness ions in dilute compartments have the trend of migrating to cation exchange membranes under effect of the direct current, which would result in high hardness concentration at the “cation membrane–solution” interface, therefore violent water splitting reaction would take place at the side of cation membranes. H^+ and OH^- ions produced by water decomposition would then enter into bulk solution of concentrate and dilute streams, thus the corresponding pH would gradually decrease and increase, respectively. In all experiments of this study, the principle of catalyzed water splitting and pH variation were similar with each other, which could be also inferred from the *pH-T* curves in Figs. 6 and 9.

In experiment A3, after decline from 8.94 to 6.27 in the second period, the concentrate pH kept stable in the later 40 hours operation instead of a continuous decrease. The reason was that more cation exchange resins were used than anion exchange resins in concentrate compartments. As the stack current continuously increased to higher than 130 mA, water decomposition occurring on surface of cation exchange membranes was severe than that on surface of anion exchange membranes, thus higher net H^+ ions would migrate into concentrate compartments, which sequentially caused the concentrate pH to decrease.

The product resistivity is directly affected by the separation force, namely the applied electric field, which could be validated from curves in Figs. 7 and 8.

After each experiment, the stack was disassembled to check the situation of precipitation. It was found that much or less precipitation occurred in each stack in concentrate compartments of the second passage, and that in stack with configuration A there was more precipitation while only a little was found in the stack with configuration C. It had been proved that configuration C has better separation

performances and stability than configuration A and B. Mixed-bed resins packing with cation proportion higher than 50% is much effective for precipitation averting.

3.3.2. Effect of flow manner of concentrate stream

Another series of experiments with serial number of B1, B2, and B3, were carried out to estimate the influence of inner water flow via three EDI stacks with configuration C, D, and E. Important conditions for these experiments were all the same as mentioned in section 2.4. The pH variation, stack currents, and product resistivities of these experiments are shown in Figs. 9, 10 and 11, respectively.

Since obvious exceptional changes of parameters directly related with precipitation, i.e. durative decrease of stack current and product resistivity, were observed, experiment B1 and B2 were terminated till 98 h and 80 h of operation, respectively.

After stack disassembly of experiment B1, some precipitation was found in concentrate compartments of

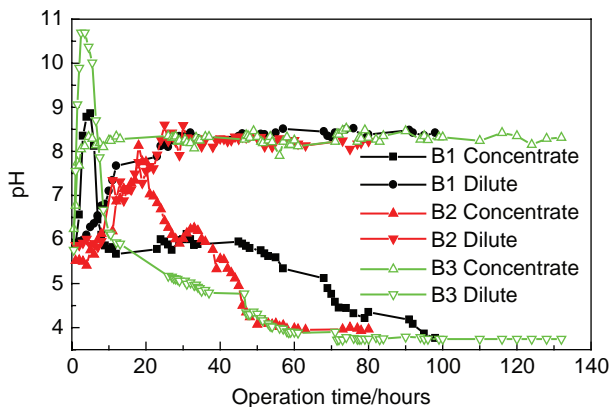


Fig. 9. pH variation versus operation time of experiments with different configurations.

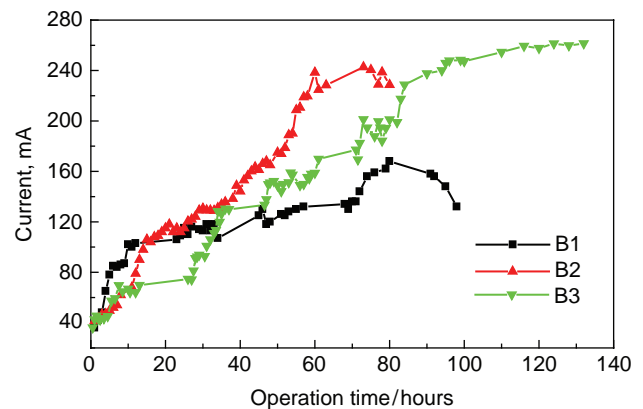


Fig. 10. Stack currents versus operation time of experiments with different configurations.

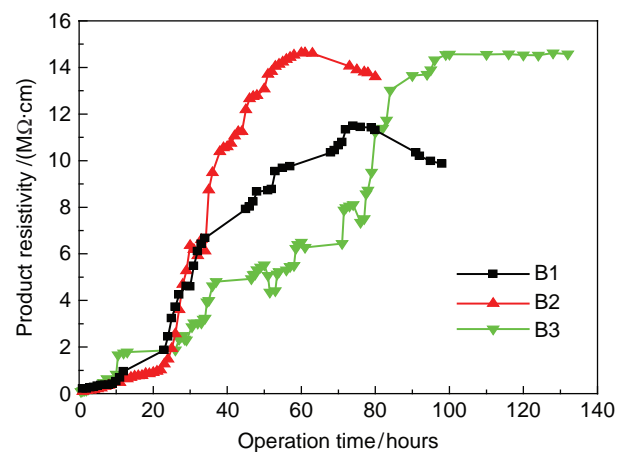


Fig. 11. Variation of product resistivity versus operation time of different stacks.

the second passage near the dilute outlet. However, as to experiment B2, just a little precipitation was found in concentrate compartments of the first passage near dilute inlet. The reason was that countercurrent of concentrate stream resulted in high hardness concentration in the compartments. The results indicated that even in dilute compartments of the first passage, water splitting reaction could not be neglected. No precipitation was observed in the second passage near the dilute outlet since the hardness ions could be effused out of the stack immediately, therefore the condition of high hardness concentration could not take place.

From Fig. 10 it can be seen that, mostly stack current of experiment B2 was higher than that of B1. Besides, similar relationship could also be observed on the resistivity–time curve in Fig. 11. Countercurrent of streams had been validated to be helpful to reduce the stack resistance.

According to Fig. 9, pH variations of these experiments were similar with each other. After 20 h operation, the out dilute pH kept stable in range of 8.0–8.6, while the concentrate pH continuously decreased to the level of 3.7–4.0. Since the feed pH was around 5.8, it could be inferred that unsymmetrical water decomposition had taken place in dilute compartments, and that which occurred on surface of cation membranes was stronger than that on surface of anion membranes.

Satisfactory results had been obtained in experiment B3 via EDI stack with configuration E. During entire operation of 132 h, both the stack current and dilute resistivity continuously increased till a maximum value of 260 mA and 14.6 MΩ·cm were obtained, respectively. Good operation stability could also be observed via the *pH-T* curve in Fig. 9, especially after 60 h operation. The stack was then disassembled after the experiment, and no precipitation was found in all the compartments. Compared with other experiments of the above two series, the improvements of packing resins in concentrate compartments and countercurrent of streams had been adequately confirmed for precipitation averting.

3.4. Characteristics and performances of the improved EDI process

3.4.1. Mass balance

Mass balance analysis is an effective criterion on whether the separation process has reached stable stage, and the major aspect should focus on the objective ions, namely balance of Ca²⁺ and Mg²⁺ ions. Fig. 12 shows the concentration variation of cation ions of the concentrate effluent in experiment B3.

Since cation exchange resins of the mixed-bed both packed in dilute and concentrate compartments was initially of Na⁺ form, the Na⁺ ion on cation resins in dilute

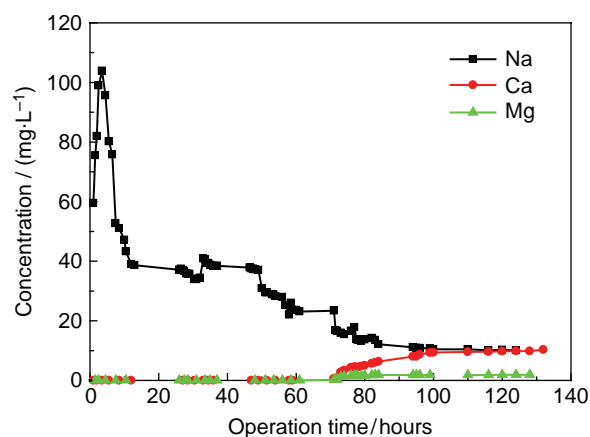


Fig. 12. Concentration variation of cation ions of the concentrate effluent in experiment B3.

compartments was then migrated into concentrate compartments under effect of applied current, therefore there was a steep peak on the concentration curve of Na⁺ in several hours after start-up. With durative operation of the process, Na⁺ ion was continuously removed from the stack, thus the Na⁺ concentration gradually decreased till the termination.

No hardness ions were observed in 70 h after start-up. The reason was that they would be first absorbed onto cation exchange resins according to principle of “preferential adsorption”. The Ca²⁺ and Mg²⁺ ions both have much greater selective coefficient on cation exchange resins than the Na⁺ ion ($K_{Na, Ca} = 3\sim 6$; $K_{Na, Mg} \cong 1.6$). The process of hardness ions preferentially migrated onto cation exchange resins was similar with that of the breakthrough of mixed-bed [11,12].

After 70 h operation, the concentration of Ca²⁺ and Mg²⁺ ions gradually increased. Until termination of experiment B3, the value reached 10.27 mg·l⁻¹ and 1.88 mg·l⁻¹, respectively. Since operation parameters all kept constantly during the experiment and the electrolyte concentration in dilute product could be neglected, therefore it was easy to estimate that the theoretic Ca²⁺ and Mg²⁺ concentration of concentrate effluent under stable status should be 17.88 mg·l⁻¹ and 6.06 mg·l⁻¹, respectively. It was obvious that the mass balance of objective ions had not been achieved yet till the termination. The adsorption equilibrium on cation exchange resins should be obtained through a much long-term process. Provided that the separation process could be continuously operated, the concentration of hardness ions would also increased accordingly.

3.4.2 Separation capabilities

Performances of the separation process could be evaluated by indexes including removal ratio (*R*), current

efficiency (η) and energy consumption (E), which were respectively defined as following [13,14]:

$$R = \frac{C_i - C_f}{C_i} \times 100\% \quad (3)$$

$$\eta = \frac{Qz(C_i - C_f)F}{N \times I} \times 100\% \quad (4)$$

$$E = \frac{V \times I}{Q} \quad (5)$$

where C_i and C_f are the concentration of dilute feed and dilute product, respectively; Q is the flow rate of dilute water, z is the valent number of metal ions, F is the Faraday constant, N is the number of cell pairs, I is the operation current, V is the applied voltage.

In experiment B3, the dilute flow rate (Q) was 30.0 l·h⁻¹, and the final product resistivity, stack voltage and current were 14.6 MΩ·cm, 30.0 V and 260 mA, respectively. The removal ratio could be approximatively calculated based on conductivities of the feed and product, therefore the removal ratio (R), current efficiency of Ca²⁺ (η_{Ca}) was calculated to be 99.8% and 11.6%, respectively, the energy consumption (E) was just 0.26 KW·h·m⁻³.

The experiments result indicated that, even with unqualified feed water with hardness of 11.7 mg·l⁻¹ (as CaCO₃), the improved EDI process could be operated to give well results similar with that of a normal EDI process followed upstream of a "RO/RO" system.

4. Conclusions

In this paper, an improved EDI configuration was put forward for precipitation averting when with unqualified feed hardness. Improvements including countercurrent of dilute and concentrate streams, mixed-bed resins filling in concentrate compartments with cation proportion higher than 50%, and shorter hydraulic retention time for concentrate stream than that of dilute stream were all helpful for the separation. Stable operation and dilute resistivity up to 14.6 MΩ·cm had been achieved in durative experiment of 130 h when with feed hardness of 11.7 mg·l⁻¹,

the hardness rejection could reach 99.8% while the energy consumption was as low as 0.26 KW·h·cm⁻³. The improved EDI process would find its wide application for pure water production in the future.

Acknowledgements

The authors gratefully appreciate the support on this work by the projects as following: National high and new technologies R&D project, China (Grant number: 2007AA06Z330) and key science research project of Tianjin, China (Grant number: 08ZCKFSH01800).

References

- [1] A.J. Giuffrida, G.C. Ganzi and O. Yoram, Electrodeionization apparatus and module, EP patent, 0379116A2, July, 25, 1990.
- [2] E.K. William, I.D. Elyanow and K.J. Sims, Electrodeionization Polarity Reversal Apparatus and Process, US Patent, 5026465, June, 25, 1991.
- [3] J. Park, J. Song, K. Yeon and S. Moon, Removal of hardness ions from tap water using electromembrane processes, *Desalination*, 202 (2007) 1–8.
- [4] D.F. Tessier, Method and apparatus for preventing scaling in electrodeionization units, US patent, 6149788, Nov. 21, 2000.
- [5] L. Fu, J. Wang and Y. Su. Removal of low concentrations of hardness ions from aqueous solutions using electrodeionization process, *Separation and Purification Technol.*, 2009, 68:390–396.
- [6] R. Simons, Strong electric field effects on proton transfer between membrane-bound amines and water, *Nature* 280 (1979) 824–826.
- [7] R. Simons, Electric field effects on proton transfer between ionizable groups and water in ion exchange membranes, *Electrochim. Acta* 29 (2) (1984) 151–158.
- [8] R. Simons, Water splitting in ion exchange membranes, *Electrochim. Acta* 30 (3) (1985) 275–282.
- [9] V.V. Ganych, V.I. Zabolotskii and N.V. Sheldeshov, Electrolytic dissociation of water molecules in systems comprising solutions and MA-40 anion-exchange membranes modified with transition metal ions, *Sov. Electrochem.*, 28 (1992) 1138–1143.
- [10] Y. Tanaka, Acceleration of water dissociation generated in an ion exchange membrane. *J. Membr. Sci.*, 303 (2007) 234–243.
- [11] M. Mozammel, S.K. Sadrezaad, E. Badami and E. Ahmadi, Breakthrough curves for adsorption and elution of rhenium in a column ion exchange system, *Hydrometallurgy*, 85 (2007) 17–23.
- [12] I. Lee, Y. Kuan and J. Chern, Prediction of ion-exchange column breakthrough curves by constant-pattern wave approach. *J. Hazard. Mat.*, 152 (2008) 241–249.
- [13] X. Feng, Z. Wu and X. Chen, Removal of metal ions from electroplating effluent by EDI process and recycle of purified water, *Separation and Purification Technol.*, 57 (2007) 255–261.
- [14] M.B.C. Elleuch, M.B. Amor and G. Pourcelly, Phosphoric acid purification by a membrane process: Electrodeionization on ion-exchange textiles. *Separation and Purification Technol.*, 51 (2006) 285–290.